Long-range correlation analysis of urban traffic data*

Sheng Peng(盛 鹏)[a)b)], Wang Jun-Feng(王俊峰)[a)b)†], Tang Tie-Qiao(唐铁桥)[c)], and Zhao Shu-Long(赵树龙)[a)b)]

[a)] *School of Computer Science, Sichuan University, Chengdu* 610064, *China*

[b)] *Key Laboratory of Fundamental Synthetic Vision Graphics and Image Science for National Defense, Sichuan University, Chengdu* 610064, *China*

[c)] *School of Transportation Science and Engineering, Beijing University of Aeronautics and Astronautics, Beijing* 100191, *China*

(Received 28 October 2009; revised manuscript received 5 December 2009)

This paper investigates urban traffic data by analysing the long-range correlation with detrended fluctuation analysis. Through a large number of real data collected by the travel time detection system in Beijing, the variation of flow in different time periods and intersections is studied. According to the long-range correlation in different time scales, it mainly discusses the effect of intersection location in road net, people activity customs and special traffic controls on urban traffic flow. As demonstrated by the obtained results, the urban traffic flow represents three-phase characters similar to highway traffic. Moreover, compared by the two groups of data obtained before and after the special traffic restrictions (vehicles with special numbered plates only run in a special workday) enforcement, it indicates that the rules not only reduce the flow but also avoid irregular fluctuation.

Keywords: urban traffic data, long-range correlation, detrended fluctuation analysis, special traffic restriction

PACC: 0250, 0560

1. Introduction

Traffic parameters such as flow and velocity are vital in real traffic. They can be used as decisive variables to determine traffic control and management strategies in real time as well as characterize road traffic congestion for further use in advanced intelligent traffic systems. Thereby, in recent decades, the research about traffic data has become a hot topic. In traffic forecasting, Jiuh presented a stochastic modeling approach to dynamic prediction of section-wide inter-lane and intra-lane traffic variables using point detector data,[1] Chrobok *et al.* proposed a heuristic method based on the statistical analysis of historical data,[2] Meng *et al.* applied a local support vector machine regression model to small-time scale network traffic prediction.[3] In traffic accident detection, Ferrer *et al.* proposed a disaggregated data approach to study the effects of policy variables, calendar events, and different seasonal behaviours.[4] In other fields, Luca *et al.* developed an information extension model (IEM) which uses location data of bus fleets to estimate road traffic conditions and provide input for implementing control strategies,[5] Xiao *et al.* studied the dynamics of the synchronous totally asymmetric simple exclusion process on lattices with two consecutive junctions in a multiple-input-multiple-output traffic system.[6] In these applications of real traffic data, their models are usually traditional statistical methods and lack of descriptions about the temporal and space complexity of traffic flow.

On the other hand, as traffic parameters are time series, some scientists concentrated on explaining the complex architectures of traffic flow by the theoretical analysis of the time scale of fluctuations in traffic data. Since Mush and Higuchi firstly found $1/f$ fluctuations in empirical data measured in traffic flow in 1976,[7] the long-range correlation has been widely used for the theoretical description of diverse phenomena in traffic flow. There exist three long-range correlated processes: antipersistent, persistent, and ordinary diffusion. An antipersistent long-range correlated process shows that a step in one direction is preferentially followed by a reversal of direction. A per-

*Project supported by the National High Technology Research and Development Program of China (Grant Nos. 2008AA01Z208 and 2009AA01Z405), the Applied Basic Research Program of Sichuan Province of China (Grant No. 2010JY0013) and the Youth Foundation of Sichuan Province of China (Grant No. 2009-28-419).

†Corresponding author. E-mail: wangjf@scu.edu.cn

© 2010 Chinese Physical Society and IOP Publishing Ltd

sistent long-range correlated process indicates that a step in one direction is preferentially followed by another step in the same direction. While in the ordinary diffusion process, each step is independent of its preceding one.[8,9] Neubert *et al.*[10] and Gao *et al.*[11] respectively proved that traffic parameters have long-range correlation in synchronized flow by autocorrelation function, Gao *et al.*[11] proposed that the power-law dynamic behaviour of the density fluctuation has different long-range correlation in free flow, synchronized flow and wide moving jam,[9] and they also studied phase transition in evolution of traffic flow with scale-free property.[12] Shang *et al.*[13] presented that highway traffic data exhibit the multi-fractal behaviour by geometrical approaches such as the Hölder exponent method. But for some reason (i.e. it needs a lot of real traffic data in different time scales), there are few studies and applications about the long-range correlation analysis of urban traffic flow.

In this paper, we firstly investigate urban traffic data by analysing the long-range correlation with detrended fluctuation analysis (DFA). Through a large number of real time data collected by the travel time detection system in Beijing, according to the difference of the long-range correlation, we study the effect of intersection location, people activity custom and special traffic controls on urban traffic flow.

The rest of the present paper is organized as follows. In Section 2, we introduce DFA method. In Section 3, compared by real traffic data, we investigate different factors on urban traffic flow. In Section 4, we discuss the performance of different DFA methods on different time scales. In Section 5, we conclude.

2. Detrended fluctuation analysis

Since Peng *et al.*[14] first proposed DFA based on random walk theory in 1994, it has been established as an important method to reliably detect long-range (auto-) correlations in data affected by trends. A major advantage of the DFA technique is the systematic elimination of polynomial trends of different order, which can assist in gaining insight into the scaling behaviour of the natural variability as well as into the kind of trends of the considered time series.[15] It was first developed for analysing the long-range correlation in DNA sequence; Kiyono *et al.*[16] employed DFA to study complex heat beat time series; Chen *et al.* investigated the scaling phenomenon of flow in complex networks;[17] Wang *et al.* used the DFA method to study the Lorenz system's long-range correlation for different initial values and parameters;[18] Hou *et al.* studied the long-range correlation of different atmosphere events by DFA;[19−21] Sheng *et al.*[22] investigated the effect of stochastic accelerating and delay probability on traffic flow by DFA. In this paper, we induce the standard DFA as follows:

(i) Start with a time series $\{x(t)\}$, $t = 1, 2, \ldots, T$, where T is the length of the time series. And integrate $\{x(t)\}$ to obtain the profile $y(t)$ of the time series defined as the accumulated deviation from the mean:

$$y(t) = \sum_{i=1}^{t} [x(i) - \langle x \rangle], \tag{1}$$

where the brackets $\langle\ \rangle$ indicate the average over the whole series of x, $\langle x \rangle = T^{-1} \sum_{i=1}^{T} [x(i)]$.

(ii) Divide the profile into int(T/l) non-overlapping segments of equal length l ('scale').

(iii) If $ml \leq t \leq (m+1)l$, then we obtain the detrend profile $y_l(t)$ by subtracting the local trend $\tilde{y}_m(t)$ in each segment:

$$y_l(t) = y(t) - \tilde{y}_m^p(t), \tag{2}$$

where $y_l(t)$ is defined by fitting the raw profile $y(t)$ in the segment. The degree of the polynomial function $y_l(t)$ can be varied in order to eliminate linear ($p = 1$), quadratic ($p = 2$) or higher order trends of the profile $y(t)$.[23] Conventionally the DFA is named after the order of the fitting polynomial (e.g. DFA-1 and DFA-2). Note that DFA-1 is equivalent to Hurst's analysis in terms of detrending. Ivanov and Chen *et al.* systematically studied the performance of different DFA methods for artificially generated signals with different trends.[24−26] Moreover, Bashana *et al.* presented a detailed comparison between the regular DFA and two recently suggested methods: the centred moving average method and a modified DFA.[15] Here we employ DFA-P ($P = 1, 2, 3, \ldots$), where the linear least square method is used to fit the profile.

(iv) The standard deviation of the detrended series is defined as the mean square of the detrended profile $y_l(t)$ on scale l:

$$F(l) = \sqrt{T^{-1} \sum_{t=1}^{T} y_l^2(t)}. \tag{3}$$

(v) Repeat this procedure with different scale l. For scale-invariant signals with power-law correlations, there is a power-law relationship between $F(l)$ and scale l:

$$F(l) \sim l^{\alpha}, \tag{4}$$

where α is the Hurst (scaling) exponent. When $0 < \alpha < 0.5$, the time series is long-range anticorrelated; when $0.5 < \alpha < 1$, it is called long-range correlation; $\alpha = 0.5$ corresponds to the Gaussian white noise; $\alpha = 1$ indicates the $1/f$ noise.

Furthermore, as proposed by Neubert *et al.*,[10] the long-range correlation of traffic parameters can be estimated by autocorrelation function. When the value of autocorrelation function is zero, it has no long-range correlation (i.e. the autocorrelation function value of synchronized flow is unequal to zero). The autocorrelation function is defined as follows:[10]

$$\alpha_x(\tau) = \frac{\langle x(t)x(t+\tau)\rangle - \langle x(t)\rangle^2}{\langle x^2(t)\rangle - \langle x(t)\rangle^2}, \qquad (5)$$

where $\{x(t)\}$ is the aggregated quantities of flow, τ is the time interval, the brackets $\langle\ \rangle$ indicate the same mean as that in the equation mentioned above.

3. Analyses and results

3.1. Traffic data collection

In our experiment, all traffic data are collected by the Beijing Travel Time Detection System based on the precise vehicle plate recognition technology. The system has more than 300 detectors distributed in the main road from the centre to the suburban. The data include a large number of single vehicle data which compose of time and velocity. In this paper, we select four intersections distributed as shown in Fig. 1. Every point has six parallel lanes, and three lanes for each direction. The direction is from east to west, and the other is converse.

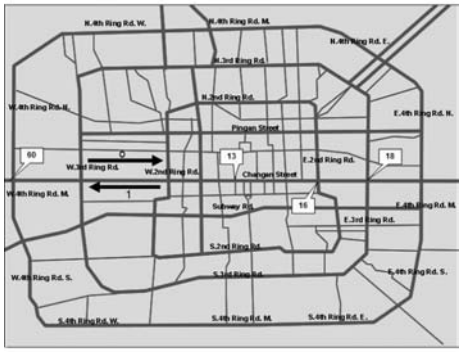


Fig. 1. The distribution map of intersection detectors. In the figure, the four detectors are in the centreline of Beijing. The No. 13 point (Fuyou Crossroad) is in the centre, and the No. 60 (Wukesong Interchange) is in the fourth ring road and is most far from the centre, and the No. 16 (Ritan Crossroad) is in the second ring road, and the No. 18 (Guomao Interchange) is in the third ring road. Besides, we define two directions: the direction 0 and the direction 1 as described by the two dark arrows in Fig. 1. The direction 0 is from west to east, and the direction 1 is converse. Apparently, for the No. 13, the No. 16 and the No. 18, the direction 0 means that drivers leave from the centre to the suburban, while direction 1 means the converse. Similarly, the directions of the No. 60 also mean the reverse.

3.2. Basic features of traffic flow in single intersection

Firstly we study the primary features of urban traffic flow. According to the real urban traffic data of Beijing, we obtain the fundamental diagram.

As shown in Fig. 2, it clearly shows that the data of flow and velocity display a wide and two-dimensional scattering. Similar to Fig. 5 in Ref. [27], it describes free flow and synchronized flow in different densities. It means that urban traffic data show some three-phase characters similar to highway traffic data.

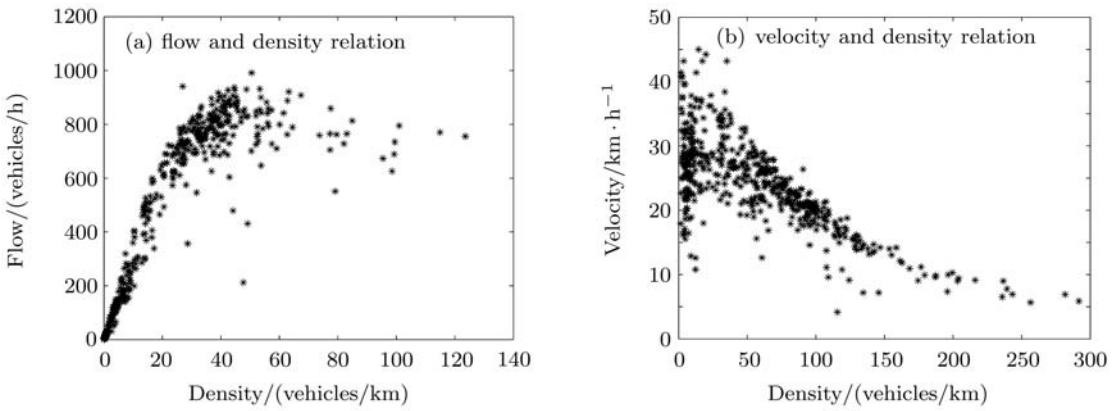


Fig. 2. The fundamental diagram.

Next, we investigate the time fluctuation of a single intersection. In the experiment, the data from the No. 16 detector (from 0:00 am to 23:59 pm on 18 June 2008). By different time scale, the time series plot of flow is demonstrated as follows.

From the diagram (a) of Fig. 3, according to the difference of the flow, we define the following three phases in real traffic flow: 1) Free time, it represents the time period when vehicles can run in a high velocity for a low density; 2) Usual daytime, it represents the time period when vehicles run in ordinary velocity; 3) Jam time, it represents the time period when a jam usually appears because of high density.

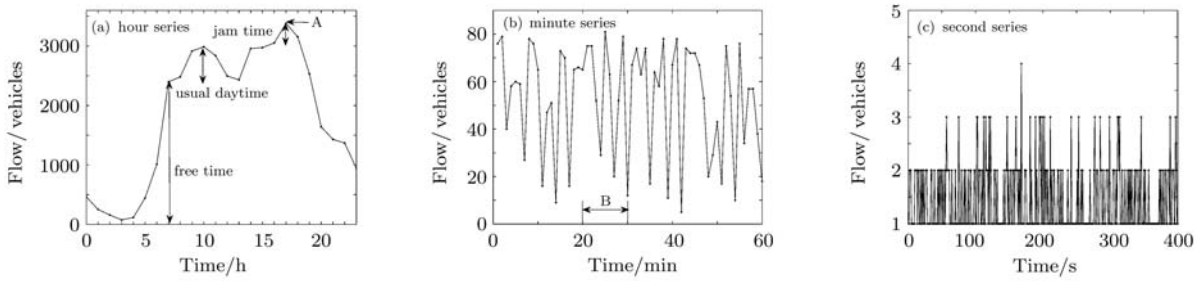


Fig. 3. The time series plot of flow. In the figure, diagram (a) shows hour series in one day, diagram (b) shows minute series in the hour marked as A in diagram (a), and diagram (c) shows second series in the period marked as B in diagram (b).

As shown in Fig. 3, from 0 am to 7 am, the flow increases with time; from 8 am to 20 pm, the flow fluctuates within a certain range, at 18 pm, it usually reaches the maximum; since 20 pm, the flow decreases with time. Apparently, it is in accord with real traffic phenomena. Moreover, compared by the three diagrams, it clearly shows that different time scales describe different characters of traffic flow. In hour scale, the time series represents the macroscopical fluctuation which is consistent with ordinary traffic trend (in rush hour, the flow usually reaches high volume); in seconds scale, it cannot describe some variation trend and its fluctuation is close to irregular noise; in minute scale, it is between them.

From Fig. 4, we can see three fluctuations of flow: the flow of free time fluctuates slightly near a low value; the flow of jam time also slightly fluctuates near a high value, and the flow of usual daytime fluctuates in a larger range than the others. It clearly shows that the three time periods represent three different phases.

And then, according to Figs. 5 and 6, we can obtain the long-range correlations of three periods. As shown in Fig. 5, the Hurst exponent α of free time and jam time is less than 0.5, while the value of usual daytime is larger than 0.5. Considering the property of the long-range correlation mentioned above and the difference of flow, similar to the conclusion proposed by Wu and Gao,[9] we indicate that the flow of free time, jam time and usual daytime respectively represent free flow ($0 < \alpha < 0.5$), wide moving jam ($0 < \alpha < 0.5$) and synchronized flow ($0.5 < \alpha < 1$).

Furthermore, from Fig. 6, the autocorrelation function values of free time and jam time are close to zero, and the value of usual daytime fluctuates between –1 and 1. It means that free time and jam time have no long-range correlation. Apparently, it complies with the conclusion obtained from Fig. 5. In addition, it also indicates that urban traffic data show some three-phase characters.

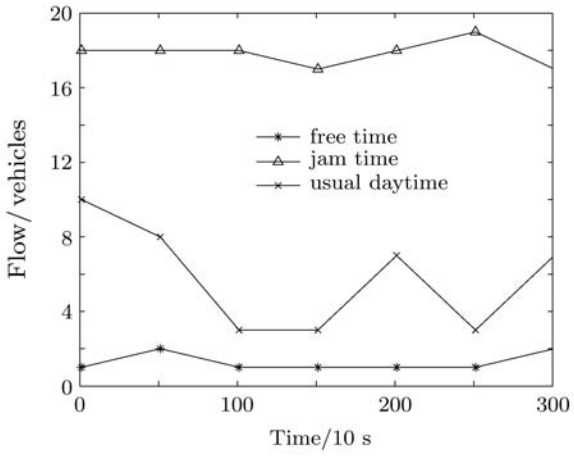


Fig. 4. The time series plot of flow in different periods. The three lines are respectively collected from three periods defined in Fig. 3: from 2 am to 4 am (free time), from 10 am to 12 am (usual daytime), and from 17:50 pm to 18:50 pm (jam time). The volume of flow is sum of the three lanes in the direction 0, and the time scale is 10 seconds.

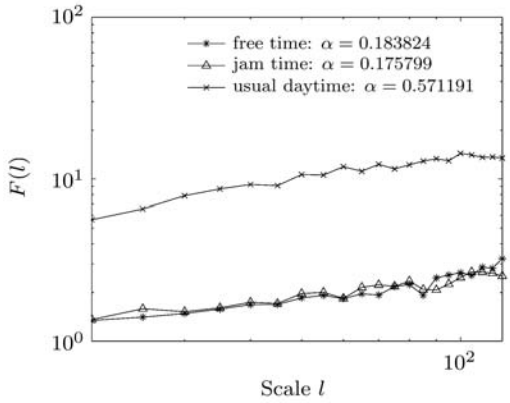


Fig. 5. The DFA of the traffic flow. The data are the same as those in Fig. 4, and the different curves represent the cases of different period similar to Fig. 4. In the legend, the average values of the Hurst exponent are listed. In the experiment, the DFA-2 is employed.

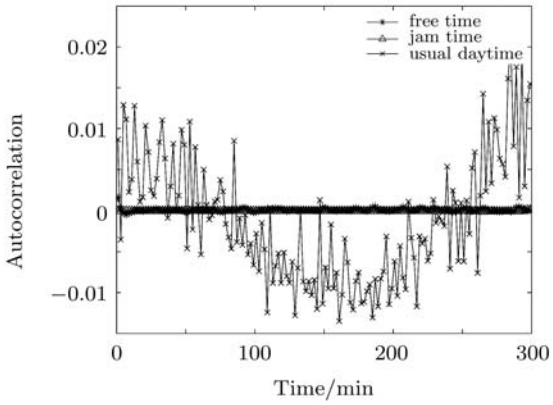


Fig. 6. The autocorrelation functions of flow. The data are the same as those in Fig. 4, and the different curves represent the cases of different periods similar to Fig. 4.

3.3. The effect of intersection location and people activity customs

In this section, we discuss the variance of flow fluctuation in different locations and directions. The data are obtained from 0:00 am to 23:59 pm on 19 June 2008.

As shown in Fig. 7, we can obtain some differences of flow as follows:

(I) In two directions, the average flow of the No. 16 is the largest and the No. 60 is the least. The flow of the No. 13 is larger than that of the No. 18. Because the No. 16 is in the second ring road, so it is the bridge node in the area between the centre and the suburban, thus its flow is larger than others.

(II) The flow of the No. 16 in the direction 1 reaches the maximum between 7 am and 8 am, while the flow of the No. 13 in the direction 0 reaches the maximum between 18 pm and 19 pm. Apparently, it is in accord with the city region characters and people activity custom. In Beijing, many people work in the centre region (usually the area within the second ring road) and live in the suburban. Thereby the flow of entering the centre is the largest in morning, and the flow of leaving is the largest in rush hours in afternoon.

(III) As the maximum flow of the No. 13 and the No. 16 is far larger than the others, in the same road capacity, it means that a jam emerges more easily in the two intersections than the others.

(IV) For the No. 60, because of the distinction of the direction about entering the centre, its flow of the direction 0 reaches the maximum at 7 am while the flow of the direction 1 reaches the maximum at 18 pm. Evidently, it is in accord with the other intersections.

To analyse the variance of the long-range correlations of traffic flow in daytime, we choose the data from 10 am to 22 pm. The volume of flow is sum of the three lanes in the same direction, and the time scale is one minute. For the period includes 10 hours, so we employ the DFA-3 in the experiment (the reason will be discussed in the following section).

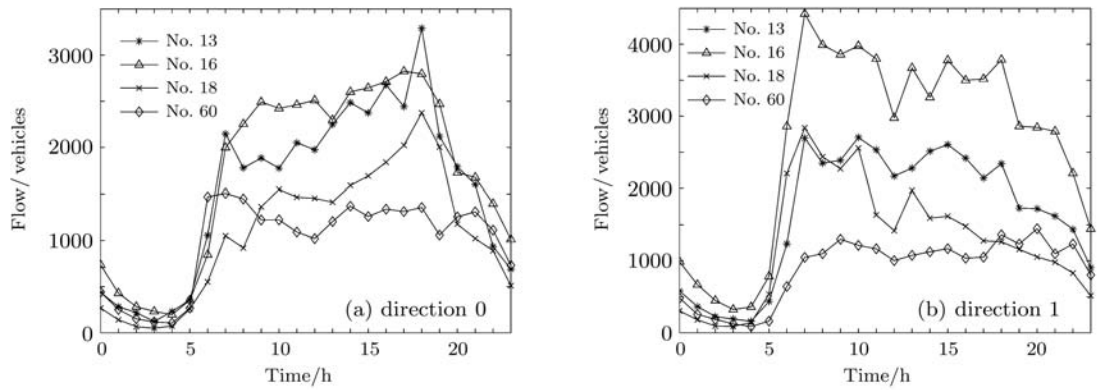


Fig. 7. The comparison of the flow of four intersections in two directions. Diagrams (a) and (b) show the flow of the direction 0 and the flow of the direction 1 respectively.

From Fig. 8, for $0.5 < \alpha < 1$, it clearly shows that the daytime traffic flows of four intersections all present long-range correlation in minute scale. Next, compared with the four diagrams, we can find out some difference of four intersections in two directions as follows:

I) In two directions, for the difference of flow discussed in Fig. 7, the exponent of the No. 13 and the No. 16 is larger than others, and the No. 60 is the least. Besides, the exponent of the direction 1 is larger than the direction 0, which is related to the difference of people activity custom mentioned above.

II) From diagrams (a) and (c), when $l < 50$, for the No. 13 and the No. 16, the exponents are close to 0.9. It means that their fluctuations tend to the $1/f$ noise. In common sense, it complies with heavy overload in the bridge nodes of the urban traffic road net.

III) According to the four diagrams, when the exponent has more irregular surges, the fluctuation function has more crossovers. Apparently, it is in accord with the relationship between the exponent and the fluctuation function.

IV) Compared with the fluctuation functions of four intersections, as the method proposed by Kantelhardt *et al.* (they proved that the correlations of recorded data do not follow the same scaling law for all time scales, but one or sometimes even more crossovers between different scaling regimes are observed),[28] we can investigate the occurrence of crossovers to detect the change of correlation behaviour in traffic flow. As shown by Fig. 8, in the two directions, when $l > 50$, the fluctuation functions of the No. 13, No. 16 and No. 18 have more crossovers (especially for the No. 13), while the No. 60 has a few crossovers.

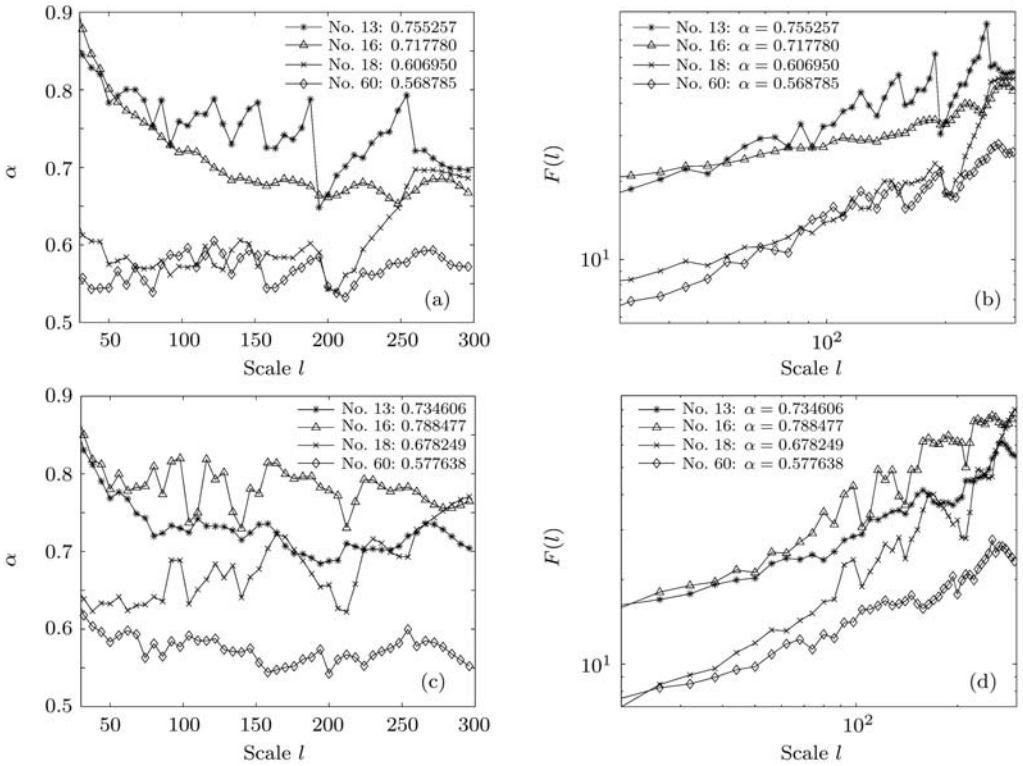


Fig. 8. The comparison of the Hurst exponent and the fluctuation function of traffic flow in daytime. Diagrams (a) and (b) show the Hurst exponent and the fluctuation function of the flow in the direction 0 respectively, and diagrams (c) and (d) show the functions in the direction 1. In the legend, the average values of the Hurst exponent are listed. In the experiment, the DFA-3 is used.

For the No. 60, it means that the traffic flow of the intersection has long-range correlation in a larger time scale than the others. Besides, according to the calm variation of flow of the No. 60 shown in Fig. 7 and the conclusions proposed by Wu *et al.*,[9] it also indicates that the flow of the No. 60 presents a synchronized flow in the most of daytime. On the other hand, for the No. 13, No. 16 and No. 18, it shows that the traffic flow has no correlation when the time scale is larger than 50 minutes. Obviously, it is consistent with some real traffic

phenomena. For example, the traffic flow of the intersection at the midtown often has different states (i.e. the correlation is diverse) in an hour ($l > 50$), thus many urban traffic forecasting applications are based on the short-term prediction models (usually 15 minutes).

3.4. The influence of special traffic controls on urban traffic flow

From 13 October 2008, for easing traffic and ensuring better air quality, within the fifth ring road, Beijing began enforcing a rule that allows only vehicles with special numbered plates on street on special day from Monday to Friday. For instance, vehicles with license plates ending with 0 and 1 are forbidden running on Monday. To study the influence of the traffic restriction on urban traffic flow, we choose 19 June 2008 (before the enforcing the rule) and 21 October 2008 for the comparison (after the enforcing the rule).

First, we analyse the variation of flow. Figure 9 shows some difference as follows: in two directions, the flows all decrease epically in rush hour (7 am and 18 pm); in the direction of entering the centre (the direction 1), for the third ring road (the No. 18), its average decrease is more than 35%, and the decrease of the second ring road (the No. 16) is about 20%. It means that the flow of entering the centre evidently reduces when the rule is employed. Namely, it also indicates that people who used to drive to work are beginning to use buses and subways. Besides, contrary to the other intersections, the decrease of the No. 60 in the direction 1 (the direction of leaving from the centre) is about –30% (i.e. the flow increases). It is the reason that people whose car is forbidden have to drive outside the fifth ring road. In general, the variation of the flow in different region distinctly describes the effect of the traffic restrictions on traffic diversion.

We then go to discuss the effect of the traffic restrictions on the traffic flow in rush hour. In real urban traffic, the flow usually reaches the maximum at 18 pm on workday, and some complex traffic phenomena (e.g. local synchronized flow pattern) often emerge at the period. So we collect the data at 18 pm on 19 June 2008 and 21 October 2008. In the experiment, the DFA-2 is used. Compared with four subplots, we can obtain the variations between 19 June 2008 and 21 October 2008 as follows: in two directions, the exponent of the No. 18 is the least; in the direction 0, the exponents of the No. 13 and the No. 16 are all close to 0.91 (namely the fluctuation trends to the $1/f$ noise) on 19 June 2008, while their values is about 0.7 on 21 October 2008; in the direction 1, the exponent of four intersections on 21 October 2008 are less than on 19 June 2008; on 21 October 2008, the exponents of the No. 18 are less than 0.5.

Finally considering these differences, we can find out that: a) when the traffic restrictions are enforced, the Hurst exponents of all intersections are lower than before; b) in the direction of leaving from the centre, for the critical intersections (such as the No. 13 and the No. 16), the fluctuations change from the $1/f$ noise to the long-range correlation (the exponent decreases from 0.91 to 0.79). According to the high outflow of synchronized flow ($0.5 < \alpha < 1$), it means that the rules effectively ease the traffic; c) in the No. 18, for $0 < \alpha < 0.5$, the traffic flow has an anticorrelated long-range correlation. As the flow is far less than the road capacity, it means that free flow of high speed appears. Namely, it has a good traffic condition in rush hour.

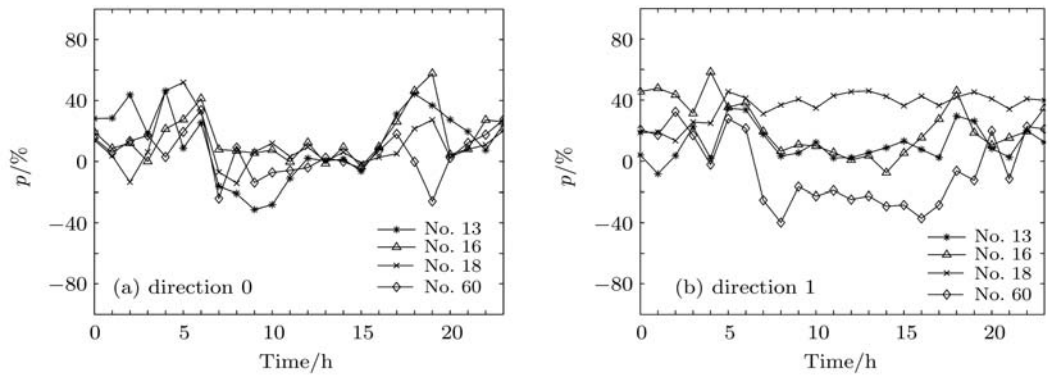


Fig. 9. The decrease proportion of flow after enforcing the traffic restrictions. Diagrams (a) and (b) show the flows of the direction 0 and the direction 1 respectively. In this figure, we define $p = 100$ ($\text{flow}_{\text{fore}}$–$\text{flow}_{\text{after}}$)/$\text{flow}_{\text{fore}}$, $\text{flow}_{\text{fore}}$ is the flow of June 19th, and $\text{flow}_{\text{after}}$ is the flow of October 21st.

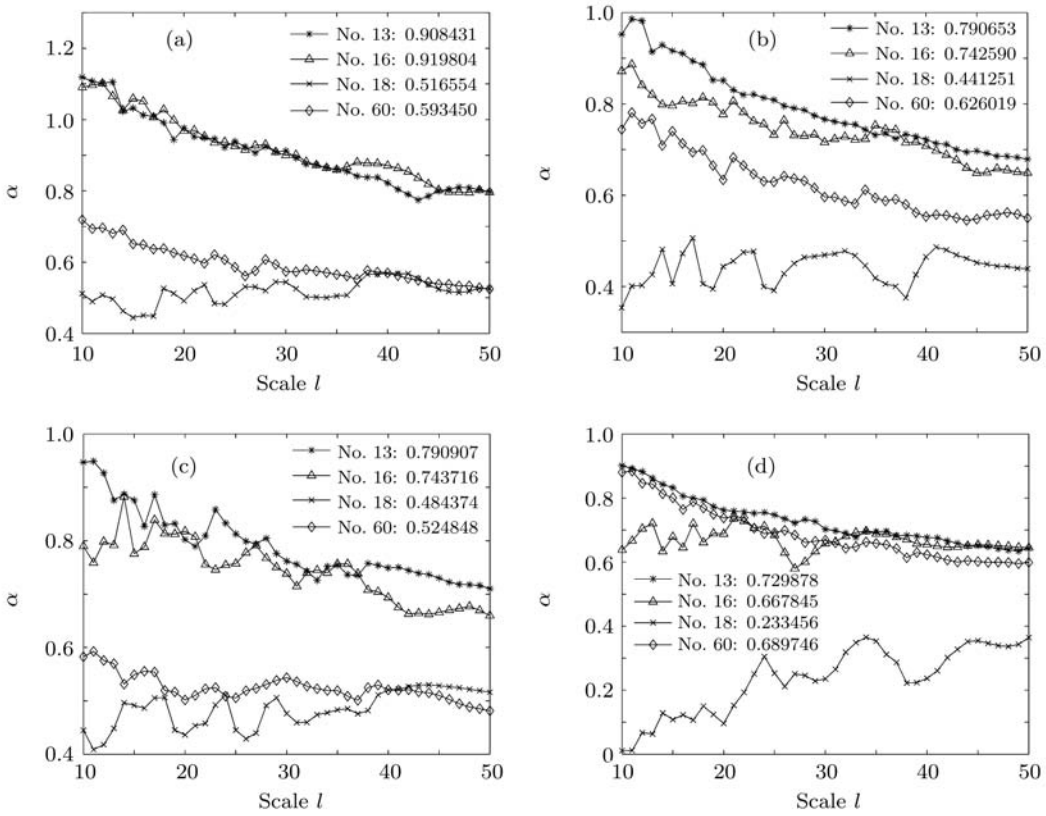


Fig. 10. The variation of the Hurst exponent after enforcing the traffic restrictions. Diagrams (a) and (b) respectively show the flows of the direction 0 and the direction 1 on 19 June 2008. Diagrams (c) and (d) respectively show the flows of the direction 0 and the direction 1 on October 21st 2008. The data were collected from 18 pm on 19 June 2008 and 21 October 2008, and the time scale is 30 seconds. In the legend, the average values of the Hurst exponent are listed. In the experiment, the DFA-2 is employed.

4. Discussions

Many real data usually exhibit different types of trends. It is clear that there is no single polynomial function that can fit perfectly all types of data. Thereby, in the detrending procedure, we should choose different DFA-P methods (appropriate order of the polynomial fit) to quantify accurately the scaling behaviour of correlated data. For example, the DFA-1 is often used to eliminate linear trend while it cannot eliminate some periodic trends. Bunde *et al.*[23] and Kantelhardt *et al.*[28] firstly presented that the appropriate order can be obtained by detecting the variation of crossover in the fluctuation function. Similarly, Xu *et al.* proposed that with the increase of several orders, the reliable order can be estimated until the change of obtained scaling exponent stops.[26] In this paper, we employ this method to obtain the order.

As shown in Fig. 3, the time series of real urban traffic have different unknown and complex trends in different scales. For obtaining credible analysis results about urban traffic data, we should choose the reliable DFA method to eliminate these trends. In this section, we discuss the performance of four DFA methods (DFA-1, DFA-2, DFA-3 and DFA-4) on different periods. The data were collected from the No. 16 on 18 June 2008 and 19 June 2008. One hour is 7 am, six hours are from 0 am to 6 am, twelve hours are from 0 am to 12 am, and fourty-eight hours include two whole day.

From Fig. 11, we can observe that: diagram (a) shows that the exponent curves of four DFA methods have similar variation when the data are short data having a weak trend. Compared with the DFA-1, the exponent of the DFA-2 is more close to the DFA-3 and DFA-4. With the method proposed by Xu *et al.*,[25] it means that the DFA-2 can accurately qualify the correlation properties of such data (e.g. the period has less than 3 hours). As shown in diagram (b), when the period is six hours, the curve of the DFA-1 is evidently different from the others. The curve of the DFA-3 and DFA-4 are homoplastic. Similarly, it is clear that the DFA-1

cannot eliminate this trend while the DFA-3 or DFA-4 can be used. Apparently, it is in accord with the periodic daily trend on scales up to 6 hours in real traffic. From diagrams (c) and (d), we also find that the higher order method should be employed when the periodic trend are more complex. However, as high order methods often have more inevitable fitting errors than others, so we should choose appropriate order in our experiment.

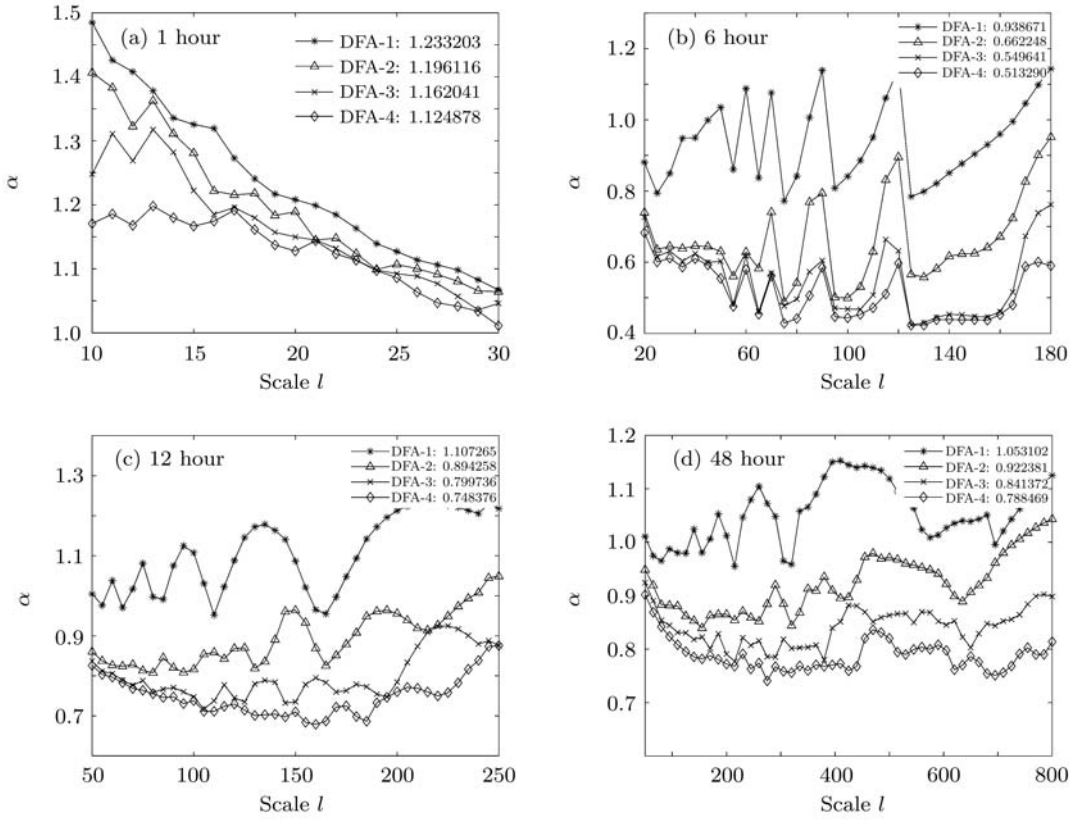


Fig. 11. The comparison of the different DFA methods in different time scales. Diagrams (a), (b), (c) and (d) respectively show one, six, twelve and fourty-eight hours. The time scale is minute. In the legend, the average values of the Hurst exponent are listed.

5. Conclusions

In this paper, through the long-range correlation analysis of urban traffic data by DFA, we investigated the effect of intersection location, people activity custom and special traffic controls on urban traffic flow. As demonstrated by our experimental results, we can draw the following conclusions: (i) the urban traffic flow represents three phases in different time periods: free flow, synchronized flow and wide moving jam; (ii) the flow of different intersection within the central area is larger than that in the suburban, and its fluctuation tends to the $1/f$ noise in rush hour; (iii) the people activity customs in workday result in different variations in two converse directions, e.g. the flow in entering centre reaches the maximum at 8 am, while the flow in leaving from centre reaches the maximum at 18 pm; (iv) the traffic restrictions not only reduce the flow, but also avoid irregular fluctuation. Compared with the two groups of real data obtained before and after the special traffic restrictions, the rule makes traffic conditions better than before.

References

[1] Jiuh B S 1999 *Trans. Res.* A **3** 79

[2] Chrobok R, Kaumann O, Wahle J and Schreckenberg M 2004 *Eur. J. Oper. Res.* **155** 558

[3] Meng Q F, Chen Y H and Peng Y H 2009 *Chin. Phys.* B **18** 2194

[4] Garca F A, Juan A D and Poncela P 2006 *Int. J. Forcasting* **22** 203.

[5] Xiao S, Cai J J, Wang R L, Liu M Z and Liu F 2009 *Chin. Phys.* B **18** 5103

[6] Luca D A, Carten A and Bruno M 2009 *Eur. J. Oper. Res.* **196** 719
[7] Musha T and Higuchi H 1976 *Jpn. J. Appl. Phys.* **15** 1271
[8] Cai S M, Yan G, Zhou T, Zhou T, Fu Z Q and Wang B H 2007 *Phys. Lett.* A **366** 14
[9] Wu J J, Sun H J and Gao Z Y 2008 *Phys. Rev.* E **78** 036103
[10] Neubert L, Santen L, Chadschneider A and Schreckenberg M 1999 *Phys. Rev.* E **60** 6480
[11] Gao K, Jiang R, Hu S X, Wang B H and Wu Q S 2007 *Phys. Rev.* E **76** 0260105
[12] Shen B and Gao Z Y 2008 *Chin. Phys.* B **17** 3284
[13] Shang P J and Shen J S 2007 *Chin. Phys.* **16** 365
[14] Peng C K, Buldyrev S V, Havlin S, Simons M, Stanley H E and Goldberger A L 1994 *Phys. Rev.* E **49** 1685
[15] Bashana A, Bartsch, Kantelhardt J W and Havlin S 2008 *Physica* A **387** 5080
[16] Kiyono K, Struzik Z R, Aoyagi N, Togo F and Yamamoto Y 2005 *Phys. Rev. Lett.* **95** 058101
[17] Chen Y D, Li L, Zhang Y and Hu J M 2009 *Chin. Phys.* B **18** 1373
[18] Wang Q G, Zhi R and Zhang Z P 2008 *Acta Phys. Sin.* **57** 5343 (in Chinese)
[19] Feng G L, Hou W and Yang P 2008 *Acta Phys. Sin.* **57** 5333 (in Chinese)
[20] Feng G L, Wang Q G, Hou W, Gong Z Q and Zhi R 2009 *Acta Phys. Sin.* **58** 2853 (in Chinese)
[21] Wang Q G, Hou W, Zheng Z H and Gao R 2009 *Acta Phys. Sin.* **58** 6640 (in Chinese)
[22] Sheng P, Zhao S L, Wang J F, Tang P and Gao L 2009 *Chin. Phys.* B **18** 3347
[23] Bunde A, Havlin S, Kantelhardt J W, Penzel T, Peter J H and Voigt K 2000 *Phys. Rev. Lett.* **85** 3736
[24] Hu K, Ivanov P C, Chen Z, Carpena P and Stanley H E 2001 *Phys. Rev.* E **64** 011114
[25] Chen Z, Ivanov P C, Hu K and Stanley H E 2002 *Phys. Rev.* E **65** 041107
[26] Xu L M, Ivanov P C, Hu K, Chen Z, Carbone A and Stanley H E 2005 *Phys. Rev.* E **71** 051101
[27] Kerner B S 2004 *Physica* A **333** 379
[28] Kantelhardt J W, Bunde E K, Rego H H A, Havlin S and Bunde A 2001 *Physica* A **295** 441